and shortening the P–N bond.[78] Although the mutually perpendicular π-components are not required to be equal by (local) symmetry, any barrier arising from their inequality is too small to have a conformational effect. Also, since the interactions of the methyl groups are attractive,[79] their deformation energies are small, so that from both causes the dimethylphosphazenes are expected to be more flexible than the hydrocarbons, as found. On the chemical time scale, differences in flexibility may become apparent. The (qualitative) rates of alkylation of $(NPF_2)_{10,12}$ appear to be very slow, the reaction of the decamer being particularly difficult to bring to completion. It is at least possible that this is a conformational effect, the phosphorus atoms in $(NPMe_2)_{10}$ being folded inward (Figure 7) more than in any other member of the series. The formation of a short transannular $CH_3\cdots F$ bond seems likely, and would need to increase the activation energy by no more than 4 kcal mol^{-1} to account for a 1000-fold decrease in rate. The structure of the dodecamer is similar but more open, and if it is unaffected by some fluorine substitution, significant retardation arising from intramolecular bonding is to be expected here also and less in the preparation of $(NPMe_2)_{11}$, as found. This may be analogous to the "medium-ring" effect described for cycloalkane derivatives many years ago;[80] structurally, Figure 13 shows the compromises necessary to optimize the steric interactions in the nonamer; in the hydrocarbon series, strain energy is maximized at the same point.

Acknowledgment. We thank the Natural Sciences and Engineering Research Council of Canada for financial support, the University of British Columbia Computing Centre for assistance, and Pat Parsons and Elizabeth Jensen for the illustrations.

Registry No. $(NPMe_2)_6$, 64651-81-6; $(NPMe_2)_7$, 64013-20-3; $(NPMe_2)_8$, 64495-80-3; $(NPMe_2)_9$, 98586-82-4; $(NPMe_2)_{10}$, 98586-83-5; $(NPMe_2)_{11}$, 98586-84-6; $(NPMe_2)_{12}$, 98586-85-7; $(NPF_2)_6$, 19258-93-6; $(NPF_2)_7$, 14616-93-4; $(NPF_2)_8$, 14097-20-2; $(NPF_2)_9$, 19258-96-9; $(NPF_2)_{10}$, 14500-76-6; $(NPF_2)_{11}$, 14097-05-3; $(NPF_2)_{12}$, 19258-99-2; MeBr, 74-83-9.

Supplementary Material Available: Table III, anisotropic thermal parameters; Table IV, calculated hydrogen coordinates and isotropic thermal parameters; Table V, measured and calculated structure factors; Table VI, bond lengths; Table VII, bond angles; Table IX, bond lengths involving hydrogen atoms; Table X, bond angles involving hydrogen atoms; Table XI, torsion angles (166 pages). Ordering information is given on any current masthead page.

(78) The role of d-orbitals in determining molecular geometry has been emphasized by: Collins, M. P. S.; Duke, B. J. *Chem. Phys. Lett.* **1976**, *42*, 364.

(79) A similar situation in inorganic high polymers has been pointed out by: Mark, J. E. *Macromolecules* **1978**, *11*, 627.

(80) (a) Kobelt, M.; Barman, P.; Prelog, V.; Ruzicka, L. *Helv. Chim. Acta* **1949**, *32*, 256. (b) Prelog, V. *J. Chem. Soc.* **1950**, 420.

Complexation of Tin(II) Chloride by a Novel Macrocycle Containing Rhodium and Nitrogen Binding Sites. The Preparation and X-ray Crystal Structure of $Rh_2Sn_2(CO)_2Cl_6[\mu$-2,6-bis(diphenylphosphino)pyridine$]_2$

Alan L. Balch,* Håkon Hope, and Fred E. Wood

Contribution from the Department of Chemistry, University of California, Davis, California 95616. *Received March 26, 1985*

Abstract: Treatment of $Rh_2(CO)_4(\mu\text{-}Cl)_2$ with 2,6-bis(diphenylphosphino)pyridine, $(Ph_2P)_2py$, in benzene forms the yellow macrocycle $Rh_2(CO)_2Cl_2[\mu\text{-}(Ph_2P)_2py]_2$ which in turn reacts with tin(II) chloride to form $Rh_2Sn_2(CO)_2Cl_6[\mu\text{-}(Ph_2P)_2py]_2$. Red crystals of $Rh_2Sn_2(CO)_2Cl_6[(Ph_2P)_2py]_2\cdot 2CH_2Cl_2$ belong to the orthorhombic space group $Pb2_1a$ (No. 29) with a = 13.959 (8) Å, b = 18.441 (10) Å, c = 25.585 (30) Å, Z = 4, R = 0.053 for 3476 reflections with $I > 4\sigma(I)$ and 450 parameters. The molecular core consists of the bent chain, Rh–Sn–Rh–$SnCl_3$. The central Sn resides within the cavity of the macrocycle and is coordinated to two nitrogen atoms, two rhodium atoms, and one chloride. In a highly uncharacteristic fashion one Sn^{II}–Cl bond has undergone oxidative addition to one of the rhodium ions.

The rigid ligand, 2,6-bis(diphenylphosphino)pyridine, $(Ph_2P)_2py$, forms a number of 12-membered macrocycles, **1**,[1,2] which have a relatively open cavity and should be capable of binding a second,

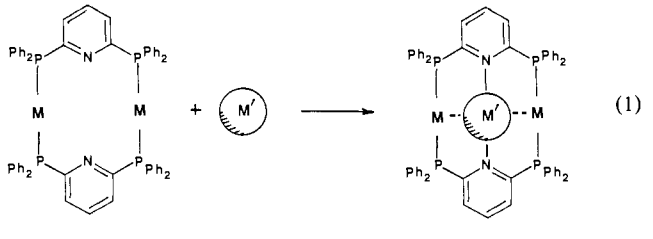

(1)

1 **2**

different metal ion in this cavity (eq 1). Complexation of this sort differs from more traditional macrocyclic chemistry[3] in that two of the potential binding sites are metal ions rather than the usual nitrogen or oxygen nucleophiles. As a consequence, metal–metal interactions will provide one of the characteristic features of the products.

Here we describe the synthesis of a macrocycle of type **1** in which M is the *trans*-Cl–Rh–CO unit. This unit prefers to bind phosphorus atoms in mutually trans orientations,[4] and coupled with the rigid nature of $(Ph_2P)_2py$, this facilitates the formation of the desired macrocycle while limiting the formation of unwanted, chelated complexes. We further demonstrate the complexation of tin(II) chloride by this macrocycle.

There is an extensive background to tin(II) chloride/groups 8–10 metal interactions, where tin(II) chloride has been used as a reductant,[5] a cocatalyst,[6] and an analytical reagent.[7] In the

(1) Wood, F. E.; Olmstead, M. M.; Balch, A. L. *J. Am. Chem. Soc.* **1983**, *105*, 6332.

(2) Wood, F. E.; Hvoslef, J.; Hope, H.; Balch, A. L. *Inorg. Chem.* **1984**, *23*, 4309.

(3) Izatt, R. M., Christensen, J. J., Eds. "Synthetic Macrocyclic Compounds"; Academic Press: New York, 1978.

(4) Sanger, A. R. *J. Chem. Soc., Chem. Commun.* **1975**, 893.

0002-7863/85/1507-6936$01.50/0

last two cases, the major function of the tin reagent has been ascribed to the formation of the $SnCl_3^-$ ligand. Numerous complexes with $SnCl_3^-$ functioning as a monodentate ligand have been isolated and structurally characterized.[8,9] In this context, binding of tin(II) to the central cavity of a macrocycle such as **1** will require it to bind in a form different from the usual $SnCl_3^-$ form.

Results

Synthetic Studies. Treatment of $(Ph_2P)_2py$ with $Rh_2(CO)_4(\mu\text{-}Cl)_2$ in benzene solution, followed by precipitation with ethyl ether, yields pale yellow crystals which contain the desired macrocycle. The infrared spectrum indicates the presence of terminal carbonyl groups at an energy (1980 cm^{-1}) consistent with the presence of *trans*-$Rh^I(CO)ClP_2$ units.[10] The yellow color is indicative of planar, noninteracting rhodium centers.[11] The ^{31}P NMR spectrum, however, shows three sets of doublets (a) δ 28.6, (J(Rh,P) = 132 Hz), (b) δ 29.3 (J(Rh,P) = 124), (c) δ 30.0 (J(Rh,P) = 127) with relative intensities (a) 4, (b) 2, (c) 1 in chloroform at 20 °C. We suspect that these arise from the cis and trans rotomeric isomers **3** and **4** and the ionic, chloro-bridged **5**. There are several other examples of restricted rotation about

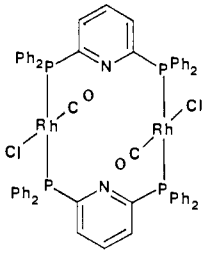

3

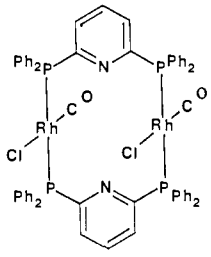

4

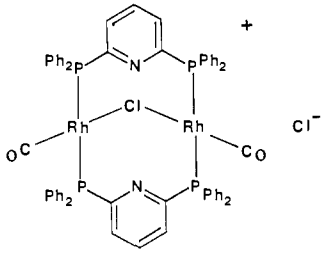

5

Rh–P bonds leading to isomers such as **3** and **4**.[12] The identification of the least intense c resonances with the chloro-bridged **5** comes from two other observations. In methanol/dichloromethane (3/2 (v/v)) the complex is a feeble conductor (30 ohm^{-1} cm^2 mol^{-1} vs. ~100 ohm^{-1} cm^2 mol^{-1} for a typical 1:1 electrolyte). Secondly, addition of 1 equiv of silver trifluoroacetate to a solution of $Rh_2(CO)_2Cl_2[\mu\text{-}(Ph_2P)_2py]_2$ yields a white precipitate and results in a ^{31}P NMR spectrum showing only the resonances reported for c above. Unfortunately, efforts to isolate the chloro-bridged cation in a pure substance have not succeeded.

The mixture of $Rh_2(CO)_2Cl_2[\mu\text{-}(Ph_2P)_2py]$ isomers has also been detected in chloroform solutions prepared by treating the structurally characterized $[Rh(CO)Cl(\mu\text{-}Ph_2Ppy)_2Rh(CO)(CH_3OH)][PF_6]$[1] with tetraethylammonium chloride. In this case the chloride ion displaces the coordinated methanol to produce the same mixture of complexes, determined by ^{31}P NMR spectroscopy, as obtained in the direct synthesis described above.

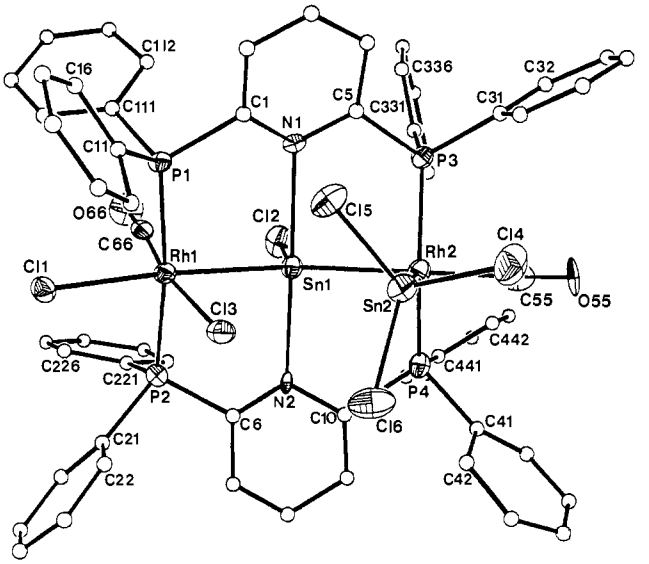

Figure 1. A perspective view of $Rh_2Sn_2(CO)_2Cl_6[\mu\text{-}(Ph_2P)_2py]_2$.

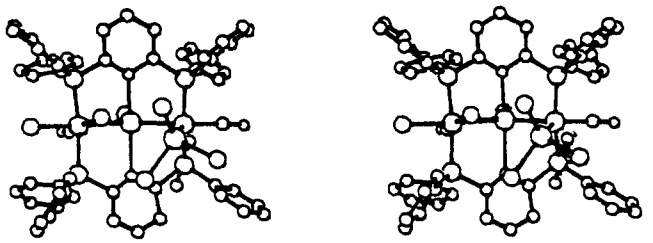

Figure 2. A stereoscopic drawing of $Rh_2Sn_2(CO)_2Cl_6[\mu\text{-}(Ph_2P)_2py]_2$.

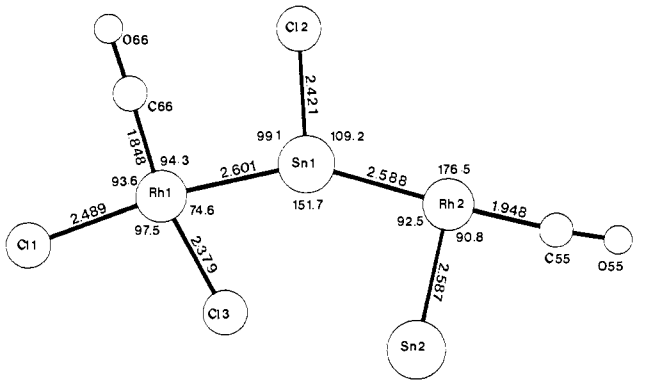

Figure 3. Some dimensions within the nearly planar cross section of $Rh_2Sn_2(CO)_2Cl_6[\mu\text{-}(Ph_2P)_2py]_2$.

The reaction between $Rh_2(CO)_2Cl_2[\mu\text{-}(Ph_2P)_2py]_2$ and 4 mol of tin(II) chloride in boiling benzene produces a purple solution from which red brown crystals of $Rh_2Sn_2(CO)_2Cl_6[\mu\text{-}(Ph_2P)_2py]_2$ were obtained in 67% yield. The ^{31}P NMR spectrum shows the presence of two types of phosphorus in the product: δ_1 42.2 pm (^1J(Rh,P) = 91.8 Hz); δ_2 67.1 (^1J(Rh,P) = 141.0 Hz) in benzene solution at 25 °C. The infrared spectrum shows two distinct terminal carbonyl stretching absorptions at 2084 and 2007 cm^{-1}. These results indicate that each of the two rhodium atoms resides in a unique environment and that one has been oxidized as shown by the markedly increased carbonyl stretching frequency (2084 cm^{-1}) and reduced ^1J(Rh,P) (91.8 Hz).

The reaction between $Rh_2(CO)_2Cl_2[\mu\text{-}(Ph_2P)py]_2$ and tin(II) chloride in benzene has been monitored by ^{31}P NMR spectroscopy. At various ratios of Rh/Sn from 2/1 to 2/4, only Rh_2-

(5) Young, J. F.; Gillard, R. D.; Wilkinson, G. *J. Chem. Soc.* **1964**, 5176.
(6) James, B. R. "Homogeneous Hydrogenation"; J. Wiley: New York, 1973. Anderson, G. K.; Clark, H. C.; Davies, J. A. *Inorg. Chem.* **1983**, *22*, 427, 434 and references in each.
(7) Walsh, T. J.; Hansman, E. A. In "Treatise on Analytical Chemistry"; Kolthoff, I. M., Elving, P. J., Eds.; Interscience: New York, 1963; Part II, Vol. 8, p 379.
(8) Young, J. F. *Adv. Inorg. Chem. Radiochem.* **1968**, *11*, 91.
(9) Zubieta, J. A.; Zuckerman, J. J. *Prog. Inorg. Chem.* **1978**, *24*, 251.
(10) Balch, A. L. *J. Am. Chem. Soc.* **1976**, *98*, 8049.
(11) Balch, A. L.; Tulyathan, B. *Inorg. Chem.* **19778** *16*, 2840.
(12) Brown, J. M.; Canning, L. R. *J. Chem. Soc., Chem. Commun.* **1983**, 460. Bushweller, C. H.; Rithner, C. D.; Butcher, D. J. *Inorg. Chem.* **1984**, *23*, 1967. Sanger, A. R. *J. Chem. Soc., Dalton* **1977**, 120.

Table I. Atomic Coordinates ($\times 10^4$) and Isotropic Thermal Parameters ($Å^2 \times 10^3$) for $Rh_2Sn_2(CO)_2Cl_6[\mu\text{-}(Ph_2P)_2py]_2 \cdot 2CH_2Cl_2$

atom	x	y	z	U	atom	x	y	z	U
Rh(1)	153 (1)	9694 (1)	8415 (1)	22 (1)[a]	C(24)	−3555 (13)	10185 (10)	9585 (7)	29 (5)
Rh(2)	4 (1)	9718 (1)	6450 (1)	25 (1)[a]	C(25)	−3051 (15)	10800 (13)	9631 (9)	46 (6)
Sn(1)	314 (1)	10000	7426 (1)	22 (1)[a]	C(26)	−2268 (12)	10950 (12)	9324 (7)	32 (5)
Sn(2)	−821 (1)	8498 (1)	6665 (1)	30 (1)[a]	C(221)	−378 (12)	11424 (10)	8816 (7)	27 (5)
P(1)	1307 (3)	8766 (2)	8401 (2)	19 (1)[a]	C(222)	−114 (15)	12018 (13)	8499 (10)	50 (6)
P(2)	−949 (3)	10628 (3)	8534 (2)	24 (2)[a]	C(223)	355 (15)	12593 (13)	8716 (9)	54 (6)
P(3)	1613 (3)	9459 (3)	6377 (2)	22 (2)[a]	C(224)	557 (14)	12619 (12)	9248 (8)	43 (6)
P(4)	−948 (3)	10727 (3)	6428 (2)	28 (2)[a]	C(225)	305 (15)	12051 (12)	9536 (9)	47 (6)
Cl(1)	−200 (3)	9305 (3)	9326 (2)	28 (1)[a]	C(226)	−132 (13)	11438 (11)	9332 (8)	34 (5)
Cl(2)	1284 (4)	11084 (3)	7494 (2)	39 (2)[a]	C(31)	1884 (12)	8891 (10)	5794 (7)	28 (5)
Cl(3)	−1073 (3)	9016 (3)	7992 (2)	28 (1)[a]	C(32)	2460 (14)	9141 (12)	5399 (7)	38 (5)
Cl(4)	−997 (4)	7658 (3)	5951 (2)	46 (2)[a]	C(33)	2554 (14)	8715 (11)	4949 (8)	38 (5)
Cl(5)	−48 (3)	7591 (2)	7190 (2)	32 (2)[a]	C(34)	2098 (13)	8077 (11)	4900 (8)	36 (5)
Cl(6)	−2453 (4)	8326 (3)	6944 (2)	48 (2)[a]	C(35)	1525 (15)	7825 (14)	5294 (9)	53 (6)
C(55)	−215 (11)	9570 (9)	5716 (7)	19 (4)	C(36)	1445 (13)	8245 (11)	5723 (8)	35 (5)
O(55)	−297 (10)	9499 (8)	5291 (5)	43 (5)[a]	C(331)	2496 (13)	10184 (10)	6372 (7)	30 (5)
C(66)	1144 (13)	10298 (11)	8615 (8)	30 (5)	C(332)	2195 (14)	10872 (11)	6235 (8)	41 (6)
O(66)	1714 (9)	10703 (8)	8756 (6)	42 (5)[a]	C(333)	2861 (15)	11431 (13)	6183 (9)	50 (6)
N(1)	1646 (8)	9010 (7)	7376 (5)	11 (3)	C(334)	3812 (18)	11267 (15)	6265 (10)	60 (7)
N(2)	−1101 (10)	10775 (8)	7490 (5)	20 (3)	C(335)	4145 (21)	10604 (16)	6381 (11)	81 (9)
C(1)	1843 (12)	8543 (11)	7763 (7)	28 (4)	C(336)	3429 (16)	10069 (14)	6436 (9)	56 (6)
C(2)	2415 (13)	7944 (11)	7713 (7)	30 (5)	C(41)	−1983 (12)	10640 (10)	6023 (7)	23 (4)
C(3)	2830 (12)	7836 (11)	7232 (7)	28 (5)	C(42)	−2659 (15)	10088 (13)	6165 (9)	53 (6)
C(4)	2667 (11)	8306 (9)	6809 (7)	22 (4)	C(43)	−3507 (18)	9978 (16)	5883 (10)	71 (8)
C(5)	2011 (11)	8876 (9)	6903 (7)	18 (4)	C(44)	−3626 (18)	10459 (14)	5448 (10)	62 (7)
C(6)	−1507 (14)	10956 (12)	7945 (8)	39 (5)	C(45)	−3014 (17)	10933 (15)	5311 (11)	67 (8)
C(7)	−2352 (13)	11376 (11)	7966 (7)	31 (5)	C(46)	−2211 (15)	11083 (14)	5598 (9)	57 (7)
C(8)	−2757 (14)	11631 (11)	7514 (8)	36 (5)	C(441)	−437 (13)	11602 (10)	6204 (8)	29 (5)
C(9)	−2332 (14)	11417 (11)	7042 (8)	37 (5)	C(442)	41 (17)	11597 (15)	5722 (11)	64 (7)
C(10)	−1529 (12)	11009 (9)	7049 (7)	22 (4)	C(443)	430 (16)	12197 (13)	5510 (10)	54 (6)
C(11)	992 (12)	7891 (10)	8668 (7)	26 (5)	C(444)	392 (14)	12847 (12)	5792 (8)	45 (6)
C(12)	66 (15)	7636 (12)	8564 (9)	40 (6)	C(445)	−74 (14)	12855 (13)	6257 (9)	47 (6)
C(13)	−119 (14)	6922 (11)	8754 (8)	35 (5)	C(446)	−487 (14)	12205 (12)	6446 (9)	40 (5)
C(14)	534 (13)	6530 (11)	9032 (8)	33 (5)	C(50)	8003 (18)	8010 (15)	9250 (11)	70 (8)
C(15)	1384 (14)	6802 (11)	9132 (8)	35 (5)	Cl(51)	7320 (6)	7900 (4)	8666 (3)	80 (3)[a]
C(16)	1664 (12)	7479 (9)	8952 (7)	20 (4)	Cl(52)	7240 (6)	7780 (4)	9779 (3)	87 (3)[a]
C(111)	2366 (12)	9085 (10)	8777 (7)	22 (4)	Cl(61)	5285 (18)	8674 (15)	7585 (9)	113 (8)
C(112)	3201 (13)	9265 (11)	8509 (8)	32 (5)	Cl(62)	4803 (18)	9892 (16)	7650 (10)	87 (8)
C(113)	3934 (13)	9546 (10)	8818 (8)	33 (5)	Cl(63)	6032 (20)	9999 (18)	7701 (12)	102 (9)
C(114)	3893 (13)	9591 (10)	9322 (7)	33 (5)	Cl(64)	4835 (30)	10662 (25)	7613 (17)	90 (12)
C(115)	3072 (12)	9372 (10)	9588 (7)	29 (5)	Cl(65)	5647 (33)	9528 (25)	7538 (17)	68 (13)
C(116)	2310 (12)	9105 (10)	9304 (7)	27 (5)	Cl(66)	6064 (36)	9063 (29)	7773 (21)	81 (14)
C(21)	−1994 (11)	10438 (10)	8971 (7)	22 (4)	Cl(67)	3808 (32)	10934 (25)	7702 (18)	65 (12)
C(22)	−2521 (11)	9835 (10)	8912 (7)	23 (4)	Cl(68)	5035 (15)	8759 (14)	7472 (9)	30 (5)
C(23)	−3298 (13)	9718 (12)	9206 (7)	36 (5)	Cl(69)	5691 (25)	10227 (20)	7775 (15)	45 (9)

[a] Equivalent isotropic U defined as one-third of the trace of the orthogonalized U_{ij} tensor.

$(CO)_2Cl_2[\mu\text{-}(Ph_2P)py]_2$ and $Rh_2Sn_2(CO)_2Cl_6[\mu\text{-}(Ph_2P)_2py]_2$ are detected. Greater amounts of the adduct are present in solutions with lower Rh/Sn ratios. The reaction is highly solvent dependent with a green solution forming in chloroform, a yellow one in ethyl acetate, and a blue one in wet acetone. The product(s) involved were not identified, and no NMR studies were conducted on these solutions.

Description of the Structure of $Rh_2Sn_2(CO)_2Cl_6[\mu\text{-}(Ph_2P)_2py]_2 \cdot 2CH_2Cl_2$. $Rh_2Sn_2(CO)_2Cl_6[\mu\text{-}(Ph_2P)_2py]_2$ crystallizes with one molecule in the asymmetric unit along with two molecules of dichloromethane, one of which is disordered. Atomic coordinates are given in Table I, and some selected interatomic distances and angles are given in Tables II and III, respectively. Figure 1 shows a perspective view, and Figure 2 shows a stereoscopic drawing of the complex. Figure 3 shows some dimensions in the nearly planar $Rh_2Sn_2(CO)_2Cl_3$ unit. Table IV presents information regarding certain planar sections within the molecule.

In the solid the complex possesses no symmetry. Each of the four metal atoms resides in a unique environment. Rh(1) is six-coordinate. Except for the angles involving Cl(3), the angles between cis pairs of ligands fall into the relatively narrow range 94.9–85.9°. Cl(3) is tilted toward Sn(1) so that the Cl(1)–Rh(1)–Cl(3) angle is opened to 97.5 (2)° and Cl(3)–Rh(1)–Sn(1) is closed to 74.6 (1)°. The O(66)–C(66)–Rh(1) group is linear. The bond distances involving Rh(1) all fall within normal limits.[13,14] The Rh(1)–Cl(1) distance is elongated relative to Rh(1)–Cl(3) and other rhodium–chlorine bond lengths as a consequence of the high trans effect of the Sn(1)–Rh(1) bond. Other examples of the structural trans effect of metal–metal bonds on metal–halogen bonds have been noted previously.[13,14]

Table II. Selected Interatomic Distances for $Rh_2Sn_2(CO)_2Cl_6[\mu\text{-}(Ph_2P)_2py]_2 \cdot 2CH_2Cl_2$

	At Rh(1)		
Rh(1)–Sn(1)	2.601 (2)	Rh(1)–P(1)	2.349 (5)
Rh(1)–P(2)	2.330 (5)	Rh(1)–Cl(1)	2.489 (5)
Rh(1)–Cl(3)	2.387 (6)	Rh(1)–C(66)	1.85 (2)
C(66)–O(66)	1.15 (2)		
	At Rh(2)		
Rh(2)–Sn(1)	2.588 (2)	Rh(2)–Sn(2)	2.587 (3)
Rh(2)–P(3)	2.304 (5)	Rh(2)–P(4)	2.288 (6)
Rh(2)–C(55)	1.92 (2)	C(55)–O(55)	1.10 (2)
	At Sn(1)		
Sn(1)–Rh(1)	2.601 (2)	Sn(1)–Rh(2)	2.588 (2)
Sn(1)–N(1)	2.62 (1)	Sn(1)–N(2)	2.42 (1)
Sn(1)–Cl(2)	2.421 (5)		
	At Sn(2)		
Sn(2)–Cl(4)	2.409 (6)	Sn(2)–Cl(5)	2.400 (5)
Sn(2)–Cl(6)	2.408 (5)	Sn(2)–Rh(2)	2.587 (3)

(13) Farr, J. P.; Olmstead, M. M.; Balch, A. L. *Inorg. Chem.* **1983**, *22*, 1229.
(14) Balch, A. L.; Guimerans, R. R.; Linehan, J.; Olmstead, M. M.; Oram, D. E. *Organometallics* **1985**, *4*, 1445.

Table III. Selected Interatomic Angles for $Rh_2Sn_2(CO)_2Cl_6[\mu\text{-}(Ph_2P)_2py]_2\cdot 2CH_2Cl_2$

	About Rh(1)		
Sn(1)-Rh(1)-P(1)	94.8 (1)	Sn(1)-Rh(1)-P(2)	91.4 (1)
P(1)-Rh(1)-P(2)	173.2 (2)	Sn(1)-Rh(1)-Cl(1)	172.1 (1)
P(1)-Rh(1)-Cl(1)	86.6 (2)	P(2)-Rh(1)-Cl(1)	87.6 (2)
Sn(1)-Rh(1)-Cl(3)	74.6 (1)	P(1)-Rh(1)-Cl(3)	95.9 (2)
P(2)-Rh(1)-Cl(3)	88.4 (2)	Cl(1)-Rh(1)-Cl(3)	97.5 (2)
Sn(1)-Rh(1)-C(66)	94.3 (6)	P(1)-Rh(1)-C(66)	86.0 (6)
P(2)-Rh(1)-C(66)	90.7 (6)	Cl(1)-Rh(1)-C(66)	93.6 (6)
Cl(3)-Rh(1)-C(66)	168.8 (6)	Rh(1)-C(66)-O(66)	175.3 (18)
	About Rh(2)		
Sn(1)-Rh(2)-P(3)	87.5 (1)	Sn(1)-Rh(2)-Sn(2)	92.5 (1)
Sn(1)-Rh(2)-P(4)	87.5 (1)	Sn(2)-Rh(2)-P(3)	105.7 (1)
P(3)-Rh(2)-P(4)	137.1 (2)	Sn(2)-Rh(2)-P(4)	117.0 (1)
Sn(2)-Rh(2)-C(55)	90.8 (5)	Sn(1)-Rh(2)-C(55)	176.5 (5)
P(4)-Rh(2)-C(55)	90.0 (5)	P(3)-Rh(2)-C(55)	92.7 (5)
Rh(2)-C(55)-O(55)	176.6 (16)		
	About Sn(1)		
N(1)-Sn(1)-N(2)	171.4 (9)	Rh(1)-Sn(1)-Rh(2)	151.7 (1)
Rh(1)-Sn(1)-Cl(2)	99.1 (1)	Rh(2)-Sn(1)-Cl(2)	109.2 (1)
Cl(2)-Sn(1)-N(2)	88.0 (5)	Cl(2)-Sn(1)-N(1)	100.5 (5)
Rh(1)-Sn(1)-N(2)	89.6 (5)	Rh(1)-Sn(1)-N(1)	87.6 (5)
Rh(2)-Sn(1)-N(2)	93.7 (5)	Rh(2)-Sn(1)-N(1)	86.0 (5)
	About Sn(2)		
Cl(4)-Sn(2)-Cl(5)	91.3 (2)	Rh(2)-Sn(2)-Cl(5)	121.7 (1)
Cl(4)-Sn(2)-Cl(6)	92.5 (2)	Rh(2)-Sn(2)-Cl(6)	126.8 (2)
		Cl(5)-Sn(2)-Cl(6)	99.7 (2)

Table IV. Selected Least-Squares Planes in $Rh_2Sn_2(CO)_2Cl_6[\mu\text{-}(Ph_2P)_2py]_2\cdot 2CH_2Cl_2$

Plane 1: N(1)C(1)-C(5)

$0.7842x + 0.5625y + 0.2619z = 16.0720$

deviations: N(1) 0.019, C(1) -0.010, C(2) -0.019, C(3) 0.001, C(4) 0.026, C(5) -0.038, P(1) 0.081, P(3) -0.221, Sn(1) -0.358 Å

Plane 2: N(2)C(6)-C(10)

$0.5605x + 0.8276y + 0.0307z = 16.164$

deviations: N(2) 0.009, C(6) 0.002, C(7) -0.017, C(8) 0.021, C(9) -0.010, C(10) -0.005, P(z) -0.016 P(4) -0.028, Sn(1) -0.072 Å

Plane 3: Rh(1)Sn(1)Cl(1)Cl(3)C(66)

$0.6375x - 0.7629y - 0.1073z = -15.827$

deviations: Rh(1) 0.016, Sn(1) -0.001, Cl(1) -0.002, Cl(3) -0.006, C(66) -0.007, O(66) -0.110 Å

Plane 4: Rh(1)P(1)P(2)Cl(3)C(66)

$0.2469x + 0.3164y - 0.9159z = -13.975$

deviations: Rh(1) -0.034, P(1) -0.145, P(2) -0.149, Cl(3) 0.137, C(66) 0.190, O(66) 0.294 Å

Plane 5: Rh(1)Sn(1)P(1)P(2)Cl(1)

$0.7221x + 0.6365y + 0.2711z = 17.327$

deviations: Rh(1) 0.043, Sn(1) -0.122, P(1) 0.110, P(2) 0.110, Cl(1) -0.138 Å

Plane 6: Rh(2)Sn(2)P(3)P(4)

$0.1349x + 0.1517y + 0.9792z = 18.9134$

deviations: Rh(2) -0.035, Sn(2) 0.009, P(3) 0.013, P(4) 0.014 Å

The environment of the five-coordinate Rh(2) is crudely but best described as trigonal bipyramidal. The Sn(1)-Rh(2)-C(55)-O(55) unit is nearly linear, while Sn(2), P(33), and P(4) reside in a plane nearly perpendicular to this unit. Thus the six angles between the axial and the equitorial ligands cluster into the range 92.8 (6)-87.4 (2)° near the ideal of 90°. However, within the Sn(2)Rh(2)P(3)P(4) plane the angular distribution is somewhat distorted so that the P(3)-Rh(2)-P(4) angle (137.4 (2)°) is opened and the Sn(2)-Rh(2)-P(3) (105.6 (2)°) and Sn(2)-Rh(2)-P(4) (116.9 (2)°) angles are closed relative to the anticipated 120°.

Sn(1) resides at the center of the macrocyclic complex. The environment of Sn(1) is also five-coordinate. It is best described as square pyramidal with Cl(2) at the apex. The Rh(1)-Sn(1)-Rh(2) angle is 151.6 (1)° and the N(1)-Sn(1)-N(2) angle is 170.8 (9)°. The two Rh-Sn distances are nearly equal while there is considerable difference between the two Sn-N distances (2.42 (1) and 2.62 (1) Å). Moreover, the longer of these is very long compared to Sn-N distances in other structurally characterized tin complexes. Although adducts of tin(II) halides with amines are known,[15] unfortunately there is no structural information available on these. The Sn^{II}-N distances that are available (2.25 (1), 2.24 (1), 2.25 (1), 2.27 (1) Å) come from tin(II) phthalocyanine.[16] Other comparisons must be made with Sn^{IV}-N distances which are expected to be shorter. Sn^{IV}-N distances as long as 2.570 (4) Å (in dimethyldiisothiocyanoto(terpyridyl)tin(IV))[17] and 2.58 (2) Å (bis[dichlorobis[2-(phenylazophenyl))tin(IV))[18] are known, but the range of Sn^{IV}-N distances is quite large.[9] For comparison with Sn(IV) in a macrocyclic environment, where these distances are the most compressed, the Sn^{IV}-N distance in (dichlorotetraphenylporphyrinato)tin(IV) is 2.098 (2)[19] Å and in (dichlorophthalocyaninato)tin(IV) the Sn^{IV}-N distances are 2.050 (3) and 2.05113 Å.[20] Nevertheless, although the Sn-N distances in $Rh_2Sn_2(CO)_2Cl_6[\mu\text{-}(Ph_2P)_2py]_2$ are at the long end of the range, it does appear that both nitrogen atoms are, in fact, bonded to Sn(1). Both pyridine rings tilt toward Sn(1). Sn(1) is clearly in the plane of the pyridine ring containing N(2), as shown by the data in Table IV. However, the geometry about the pyridine ring involved with the long Sn(1)-N(1) distance is more distorted. Both Sn(1) and P(3) show significant out-of-plane deviations (0.36 and 0.22 Å, respectively.) Thus the Sn(1)-N(1) bonding, while present, may be weak.

Sn(2) is part of a normal trichlorotin(II) ligand. Although no other Rh-$SnCl_3$ unit has been structurally characterized, one can find other examples of complexes of groups 8-10 for comparison.[8,9] The Cl-Sn-Cl angles are all smaller than the idealized 109.5° while the Rh-Sn-Cl angles are larger. The same feature is seen for other $SnCl_3^-$ complexes and for the Cl-Sn-Cl angles for noncoordinated $SnCl_3^-$ as well.[8,9]

In most complexes with bi- and tridentate bridging phosphine ligands, the phosphines are aligned trans to one another with linear P-M-P units.[21,22] However, for $Rh_2Sn_2(CO)_2Cl_6[\mu\text{-}(Ph_2P)_2py]_2$ the P-Rh-P and N-Sn-N units show varying degrees of bending. The two phosphorus atoms at Rh(1) are nearly trans (with P(1)-Rh(1)-P(2) = 173.2 (2)°). However, at Sn(1) the N(1)-Sn(1)-N(2) group is more severly bent (170.8 (9)°) and as a consequence the pyridine rings are tilted so that the nitrogen atoms point toward Sn(1). At Rh(2), the P(3)-Rh(2)-P(4) bend (137.4 (2)°) is even more substantial. Notice from Figure 2 that the direction of this bend is opposite to that at the N(1)-Sn(1)-N(2) group. The PpyP units are nearly planar except for the deviations of P(3) noted above, and there appears to be little angular distortion within these units.

Discussion

The structural results demonstrate the complexing ability of a macrocycle with rhodium and pyridine binding sites. The coordination geometry and ligation of the central tin in the product are clearly distinct from that in other tin complexes derived from tin(II) chloride.

In the formation of $Rh_2Sn_2(CO)_2Cl_6[\mu\text{-}(Ph_2P)_2py]_2$, one tin-chloride bond has added to Rh(1), which appears as a 6-coordinate 18-electron Rh(III) center. In formal terms, the central tin, Sn(1), is an Sn(0) center which acts as a two-electron donor toward Rh(1). The Rh(2) atom is five-coordinate with spectroscopic properties (ν(CO), ^1J(Rh,P)) consistent with an Rh(I) formulation. The nature of the Rh(2)-Sn(1) interaction is ambiguous. The

(15) Hsu, C. C.; Geanangel, R. A. *Inorg. Chem.* **1980**, *19*, 110.
(16) Friedel, M. K.; Hoskins, B. F.; Martin, R. L.; Mason, S. A. *J. Chem. Soc., Chem. Commun.* **1970**, 400.
(17) Naik, D. V.; Scheidt, W. R. *Inorg. Chem.* **1973**, *12*, 272.
(18) Chadra, S. L.; Harrison, P. G.; Moloy, K. C. *J. Organomet. Chem.* **1980**, *202*, 247.
(19) Collins, D. M.; Scheidt, W. R.; Hoard, J. L. *J. Am. Chem. Soc.* **1974**, *96*, 6689.
(20) Rogers, D.; Osborn, R. S. *J. Chem. Soc., Chem. Commun.* **1971**, 840.
(21) Balch, A. L. In "Homogeneous Catalysis with Metal Phosphine Complexes"; Pignolet, L. H., Ed.; Plenum Press: New York, 1983; p 17.
(22) Puddephatt, R. J. *Chem. Soc. Rev.* **1983**, *12*, 99.

Rh(2)–Sn(1) distance is almost identical with the Rh(1)–Sn(1) and Rh(2)–Sn(2) distances. Therefore it appears that there is a single bond between Rh(2) and Sn(1). If Sn(1) acts as a two-electron donor toward Rh(2), then Rh(2) achieves an 18-electron count while Sn(1) has ten valence electrons. Alternatively, Rh(2) could act as a two-electron donor toward Sn(1); this would give Rh(2) a 16-electron count while Sn(1) would have 12 electrons with an unused lone pair.

Clearly, there is a complicated network of donor–acceptor interactions operating within the core of this molecule and these interactions serve to stabilize an unusual environment for Sn(1). This sort of array of complementary donor–acceptor interactions is likely to be a distinctive characteristic of macrocycles bearing both metal centers and conventional Lewis bases as binding sites. With d^8 metal centers such as Rh(I), possessing both donor properties, due to the filled d_{z^2} orbitals, and acceptor properties, due to the collinear, empty p_z orbital, the interior of these macrocycles can assume acid or base character. Thus they can be considered to be amphoteric macrocycles and as such complement the classical nucleophilic macrocycles[3] and the less studied electrophilic macrocycles.[23] Another example of the array of donor–acceptor interactions likely to exist within such amphoteric cavities is presented by $[Rh(CO)Cl(\mu\text{-}(Ph_2P)_2py)_2Rh(CO)(HOCH_3)]^+$, **6**, which has been previously structurally characterized.[1] In this cation a methanol molecule is bound within the cavity. It is bound as a nucleophile by one electrophilic rhodium. It also acts as a hydrogen bond donor toward one of the pyridine groups. Although alcohols as solvents are believed to act as ligands toward certain Rh(I) homogeneous hydrogenation catalysts, the resulting rhodium–alcohol complexes are generally too unstable to be isolated.[24] In **6** a combination of acid/base interactions has stabilized the methanol–rhodium bonding.

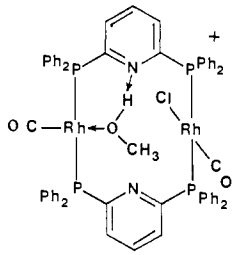

6

The rhodium macrocycle, $Rh_2(CO)_2Cl_2[\mu\text{-}(Ph_2P)_2py]_2$, has induced the tin(II) chloride to react in a highly uncharacteristic fashion. Oxidative additions of Sn^{IV}–Cl bonds to groups 8–10 metals are well established.[25] However, tin(II) generally behaves as a reductant, not an oxidant, toward these metals.[5] This sort of induced oxidative addition has been encountered previously in reactions involving (2-(diphenylphosphino)pyridine – (Ph_2Ppy)) complexes of groups 8–10 metals. For example, bis(benzonitrile)palladium(II) chloride reacts with $Rh(CO)Cl(Ph_2Ppy)_2$ and with $Ru(CO)_3(Ph_2Ppy)_2$ to form $Rh(CO)Cl_2(\mu\text{-}(Ph_2Ppy)_2PdCl$[13] and $Ru(CO)_2Cl(\mu\text{-}Ph_2Ppy)_2PdCl$,[26] respectively. In both cases Pd^{II}–Cl bonds have been added to either Rh(I) or Ru(0) centers. In these cases, we have ascribed this behavior to the severe constraints of the bridging ligands which force the two metal atoms close together. Similar constraints are present with $(Ph_2P)_2py$ as a bridging ligand. However, in the present context it is interesting to note that only one of the two Sn^{II}–Cl bonds has undergone oxidative addition to rhodium and that the two Sn(1)–Rh interactions with the complex are fundamentally different.

Table V. Summary of Crystal Parameters, Data Collection, and Refinement for $[\mu\text{-}(Ph_2P)_2py]_2Rh_2Sn_2(CO)_2Cl_6\cdot 2CH_2Cl_2$

formula	$C_{60}H_{46}Cl_6N_2O_2P_4Rh_2Sn_2\cdot 2CH_2Cl_2$
fw	1734.2
a, Å	13.959 (8)
b, Å	18.441 (10)
c, Å	25.585 (30)
V, Å	6605.8
Z	4
density, g/cm^3	1.74 (calcd, 140 K)
	1.70 (exptl, 298 K)[a]
space group	$Pb2_{1a}$ (a nonstandard setting of no. 29)
crystal dimens, mm	0.06 × 0.58 × 1.25
crystal color	dark red
radiation	Mo Kα (λ = 0.71069 Å)
temp, K	140
μ, cm^{-1}	17.36
absorp. corr. fac.	3.87–4.71
2θ max, deg	45
scan type	ω
scan speed, deg/min	10.0
scan range, deg	2.2
backgrounds	see text
refl. betw. ck. refl.	198
no. ck. refl.	2
uniq. data meas.	4191
data used ($I > 4\sigma(I)$)	3476
no. of var.	450
max. shift/esd	0.073
G.O.F.	1.86
R	0.049
R_w	0.050

Experimental Section

Preparation of Compounds. $(Ph_2P)py$ was prepared as previously described.[27]

$Rh_2(CO)_2Cl_2[\mu\text{-}(Ph_2P)_2py]_2$. A solution of 1.20 g (2.67 mmol) of $(Ph_2P)_2py$ in 15 mL of benzene was added to a solution of 0.52 g (1.34 mmol) of $Rh_2(CO)_4(\mu\text{-}Cl)_2$ in 10 mL of benzene. The solution quickly changed color from light red to yellow with the concomitant effervescence of carbon monoxide. After gas evolution ceased, ethyl ether was gradually added. The light yellow, flocculent solid was collected by filtration, washed with ether, and quickly recrystallized from dichloromethane/ether (yield 97%). Anal. Calcd for $C_{30}H_{23}ClNOP_2Rh$: C, 58.70; H, 3.78; N, 2.28; Cl, 5.78. Found: C, 58.27; H, 3.84; N, 2.26; Cl, 5.86.

$Rh_2Sn_2(CO)_2Cl_6[\mu\text{-}(Ph_2P)_2py]_2$. A solution of 0.145 g (0.822 mmol) of anhydrous tin(II) chloride in 100 mL of benzene was added to a solution of 0.252 g (0.206 mmol) of $Rh_2(CO)_2Cl_2[\mu\text{-}(Ph_2P)_2py]_2$ in 50 mL of benzene. The dark purple solution was heated under reflux for 2 h and then concentrated to 25 mL through rotary evaporation. Acetone (50 mL) was added to the mixture. Upon cooling to 0 °C, a dark red-brown microcrystalline solid was obtained. This was collected by filtration and washed with acetone. Purification was achieved by dissolving the product in a minimum of dichloromethane and filtering and then cooling the solution to −75 °C. After recovering the product by filtration, followed by vacuum drying, the yield of the solid, crystalline material was 67%.

X-ray Data Collection and Structure Determination. Dark red crystals of $Rh_2Sn_2(CO)_2Cl_6[\mu\text{-}(Ph_2P)_2py]_2\cdot 2CH_2Cl_2$ were obtained by slow vapor diffusion of ethyl ether into a dichloromethane solution of the complex. A large crystal with the shape of a flaked arrowhead (0.58 mm at the base, 1.25 long, and 0.06 mm thick) was the best that could be found. All X-ray data were obtained at 140 K on a Syntex (Nicolet) $P2_1$ diffractometer equipped with an LT-1 gas stream cooling device which was locally modified for satisfactory performance. A summary of data acquisition and structure refinement parameters is given in Table V. The systematic absences of $0kl$ for k odd and $hk0$ for h odd are consistent with the space groups $Pb2_{1a}$ and $Pbma$; the structure is consistent with $Pb2_{1a}$ (a nonstandard setting of No. 29).

The crystal was of poor quality, with ω peak scan widths in the range 2.5–3°, making it impossible to scan an entire peak without picking up intensity from neighboring reflections. Intensities were measured with 2.2° ω scans; backgrounds were recorded separately, as described pre-

(23) Azuma, Y.; Newcomb, M. *Organometallics* **1984**, *3*, 9.
(24) Stults, B. R.; Friedman, R. M.; Koenig, K., Knowles, W.; Greeyor, R. B.; Lytle, F. W. *J. Am. Chem. Soc.* **1981**, *103*, 3235. Halpern, J.; Riley, D. P.; Chan, A. S. C.; Pluth, J. J. *J. Am. Chem. Soc.* **1977**, *99*, 8055. Schrock, R. R.; Osborn, J. A. *J. Am. Chem. Soc.* **1976**, *98*, 2134.
(25) Butler, G.; Eaborn, C.; Pidcock, A. J. *Organomet. Chem.* **1980**, *185*, 367 and references therein.
(26) Maisonnet, A.; Farr, J. P.; Olmstead, M. M.; Hunt, C. T.; Balch, A. L. *Inorg. Chem.* **1982**, *21*, 3961.
(27) Newkome, G. P.; Hager, D. C. *J. Org. Chem.* **1978**, *43*, 947.

viously.[2] Two check reflections remained stable throughout data collection. Because of uncertainty in background levels, which affected weak reflections most seriously, only data with $I > 4\sigma(I)$ were included in later calculations.

The positions of the two rhodium atoms and one tin atom were determined by direct methods. The remaining atoms, except for hydrogen, were located on successive difference maps. Two solvent molecules were found, one well behaved and the other with signs of severe disorder. The disordered molecule was included as nine chlorine atom fragments, with occupancy factors from 0.15 to 0.4. No peak here could be reasonably attributed to carbon.

Following convergence of refinement with isotropic temperature factors, an empirical absorption correction was applied.[28] Final refinements were carried out with anisitropic temperature factors for all atoms heavier than nitrogen, with the exception of the disordered chlorine atoms. Hydrogen atoms were included in calculated positions. The chirality of the crystal was determined by comparing R and goodness of fit for the two "hands"; the reference parameters were obtained from a refinement with all f'' set to 0.

Final block-cascade refinement of 450 parameters converged with $R = 0.049$, average positional esd's for Rh, Sn 0.002; P, Cl 0.004; C, N, O 0.01–0.015 Å. A final difference map showed a peak of 1.4 eÅ^{-1} near Rh(2) and some smaller peaks (~0.5 eÅ^{-1}) in the region of the disordered solvent molecule.

All calculations were carried out on a Data General Eclipse computer, with local programs for data reduction and absorption correction[28] and SHELXTL for solution, refinement, molecular geometry, and graphics. The form factors, including anomalous scattering, were from the International Tables.[29]

Acknowledgment. We thank the National Science Foundation (CHE 8217954) for support. F.E.W. was a University of California Regents Fellow.

Registry No. 3, 98652-01-8; **4**, 98717-42-1; **5**, 98652-02-9; **6**, PF_6, 87555-69-9; $Rh_2(CO)_4(\mu\text{-}Cl)_2$, 14523-22-9; $Rh_2Sn_2(CO)_2Cl_6[\mu\text{-}(Ph_2P)_2py]_2$, 98653-03-0; $Rh_2Sn_2(CO)_2Cl_6[\mu\text{-}(Ph_2P)_2py]_2\cdot 2CH_2Cl_2$, 98719-05-2; $SnCl_2$, 7772-99-8; $(Ph_2P)_2py$, 64741-27-1.

Supplementary Material Available: Tables of structure factors, atomic thermal parameters, and hydrogen coordinates for $Rh_2Sn_2(Co)_2Cl_6[\mu\text{-}(Ph_2P)_2py]_2\cdot 1.5CH_2Cl_2$ (26 pages). Ordering information is given on any current masthead page.

(28) The method obtains an empirical absorption tensor from an expression relating F_o and F_c. Hope, H.; Moezzi, B., local program XABS.
(29) "International Tables for X-ray Crystallography"; Kynock Press: Birmingham, England, 1974; Vol. IV.

Mechanistic Polyoxoanion Chemistry: Intramolecular Rearrangements of the α-$Mo_8O_{26}^{4-}$, $C_6H_5AsMo_7O_{25}^{4-}$, and $(C_6H_5As)_2Mo_6O_{24}^{4-}$ Anions[1]

W. G. Klemperer,* C. Schwartz, and D. A. Wright

Contribution from the School of Chemical Sciences, University of Illinois, Urbana, Illinois 61801. *Received April 1, 1985*

Abstract: The dynamic behavior of the α-$Mo_8O_{26}^{4-}$, $C_6H_5AsMo_7O_{25}^{4-}$, and $(C_6H_5As)_2Mo_6O_{24}^{4-}$ anions as $(n\text{-}C_4H_9)_4N^+$ salts in CH_3CN has been studied by using variable-temperature ^{17}O NMR line-shape analysis, ^{17}O spin saturation transfer techniques, and ^{17}O label crossover experiments. The $C_6H_5AsMo_7O_{25}^{4-}$ anion shows two distinct types of fluxional behavior that can be related to the anion's structure, a puckered Mo_6O_{18} ring capped on opposite sides by tridentate tetrahedral MoO_4^{2-} and $C_6H_5AsO_3^{2-}$ units. The low-temperature process involves Mo_6O_{18} ring inversion accompanied by twisting of the $C_6H_5AsO_3^{2-}$ subunit and twisting or flipping of the MoO_4^{2-} subunit. Only weak (>2.2 Å) molybdenum–oxygen bonds are broken and reformed. The higher temperature process, although mechanistically undefined, involves cleavage of stronger (1.7–2.0 Å) molybdenum–oxygen bonds. Evidence is presented for related processes in the α-$Mo_8O_{26}^{4-}$ and $(C_6H_5As)_2Mo_6O_{24}^{4-}$ anions. Possibilities for observing related ring inversions and reorientations of tetrahedral subunits in other early transition-metal polyoxoanions are also discussed.

Almost nothing is known about the detailed reaction mechanisms of early transition-metal polyoxoanion transformations.[2] Despite extensive speculation on the subject, little experimental information is available due to the problem of applying standard mechanistic probes to systems of such great structural complexity. This problem is compounded by the difficulty of synthesizing specific compounds designed to test mechanistic hypotheses. The research reported here partially remedies this situation through the application of ^{17}O dynamic NMR line-shape analysis, ^{17}O spin saturation transfer techniques, and ^{17}O label crossover experiments to mechanistic polyoxoanion chemistry.

The title anions were selected for study on the basis of their common $[(RXO_3^{2-})_2(Mo_6O_{18})]$ structure, **1**, in which RXO_3^{2-} units are tetrahedral $C_6H_5AsO_3^{2-}$ and/or $OMoO_3^{2-}$ anions connected by weak molybdenum–oxygen bonds to opposite sides of an $Mo_6^{VI}O_{18}$ ring. The two key features of structure **1**, its

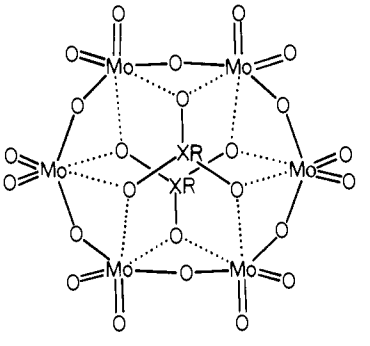

1

tetrahedral oxoanion and neutral Mo_nO_{3n} ring subunits, are of central importance since they are features observed in numerous other early transition-metal polyoxoanion structures. The tetrahedral PO_4^{3-} ion, for example, is a subunit of the Keggin anion

(1) ^{17}O Nuclear Magnetic Resonance Spectroscopy of Polyoxometalates. 3.
(2) Pope, M. T. "Heteropoly and Isopoly Oxometalates"; Springer-Verlag: New York, 1983; pp 136–140.

0002-7863/85/1507-6941$01.50/0